Biochimica et Biophysica Acta, 1101 (1992) 48–56

BBABIO 43624

Ferredoxin and flavodoxin from the cyanobacterium *Synechocystis* sp PCC 6803

Hervé Bottin and Bernard Lagoutte

Service de Bioénergétique (URA CNRS 1290), DBCM, CE de Saclay, Gif sur Yvette (France)

(Received 7 January 1992)

Key words: Cyanobacterium; Ferredoxin; Flavodoxin; Amino acid sequence; Midpoint redox potential; Isoelectric point; Iron deficiency; (*Synechocystis*)

The unicellular cyanobacterium *Synechocystis* sp PCC 6803 is capable of synthesizing two different Photosystem-I electron acceptors, ferredoxin and flavodoxin. Under normal growth conditions a [2Fe-2S] ferredoxin was recovered and purified to homogeneity. The complete amino-acid sequence of this protein was established. The isoelectric point (pI = 3.48), midpoint redox potential (E_m = −0.412 V) and stability under denaturing conditions were also determined. This ferredoxin exhibits an unusual electrophoretic behavior, resulting in a very low apparent molecular mass between 2 and 3.5 kDa, even in the presence of high concentrations of urea. However, a molecular mass of 10232 Da (apo-ferredoxin) is calculated from the sequence. Free thiol assays indicate the presence of a disulfide bridge in this protein. A small amount of ferredoxin was also found in another fraction during the purification procedure. The amino-acid sequence and properties of this minor ferredoxin were similar to those of the major ferredoxin. However, its solubility in ammonium sulfate and its reactivity with antibodies directed against spinach ferredoxin were different. Traces of flavodoxin were also recovered from the same fraction. The amount of flavodoxin was dramatically increased under iron-deficient growth conditions. An acidic isoelectric point was measured (pI = 3.76), close to that of ferredoxin. The midpoint redox potentials of flavodoxin are E_{m1} = −0.433 V and E_{m2} = −0.238 V at pH 7.8. Sequence comparison based on the 42 N-terminal amino acids indicates that *Synechocystis* 6803 flavodoxin most likely belongs to the long-chain class, despite an apparent molecular mass of 15 kDa determined by SDS-PAGE.

Introduction

The [2Fe-2S] chloroplast-type ferredoxins are distributed in various oxygenic photosynthetic organisms. They are small, strongly acidic proteins with related amino-acid sequences, having a molecular mass of about 11 kDa. They function as an electron acceptor to Photosystem-I, as well as an electron donor in many metabolic pathways [1]. Numerous amino-acid sequences of ferredoxins have been determined in a wide range of higher plants and cyanobacteria, and X-ray crystallography has provided the high-resolution structure of three cyanobacterial ferredoxins from *Spirulina platensis* [2,3], *Aphanothece sacrum* [4] and *Anabaena* sp PCC 7120 [5]. The three-dimensional structures of these proteins are largely similar, and the most conserved amino acids are mainly found in the region surrounding the iron-sulfur cluster. Midpoint potentials of cyanobacterial ferredoxins vary between −310 mV and −455 mV depending upon species [6].

The occurrence of two different ferredoxin isoforms (Fd I and Fd II) in some cyanobacteria is now clearly demonstrated. They can be distinguished by amino acid sequences and may also have different midpoint redox potentials and charges [6–8]. Ferredoxin isoproteins have also been detected in higher plants [9–12]. The relative amounts of the two ferredoxins differ greatly between species and also according to the development stage in higher plants.

Flavodoxins are low-molecular-mass (14–23 kDa) FMN-containing proteins mediating low-potential electron transfer in prokaryotes and some eukaryotic algae [6,13]. They can be divided in two classes according to their molecular mass, with one class in the 14–17 kDa range (found in anaerobic bacteria, except *Rhodospirillum rubrum*), and the other in the 20–23 kDa range

Abbreviations: DTNB, 5,5′-dithiobis(2-nitrobenzoic acid); Fd, ferredoxin; Fd_p, precipitating ferredoxin; Fd_s, soluble ferredoxin; FMN, riboflavin 5′-phosphate (flavin mono-nucleotide); FPLC, fast protein liquid chromatography; HPLC, high-pressure liquid chromatography; PE-apo-Fd, *S*-pyridylethylcysteinyl-apo-ferredoxin; SDS-PAGE, sodium dodecyl sulfate polyacrylamide gel electrophoresis; TFA, trifluoroacetic acid.

Correspondence: H. Bottin, Service de Bioénergétique (URA CNRS 1290), DBCM, CE de Saclay, 91191 Gif Sur Yvette Cedex, France.

(found in cyanobacteria, some green and red algae). FMN is the redox prosthetic group of flavodoxin, and is not covalently attached to the protein. The midpoint potentials of flavodoxins semiquinone/quinol transition (semi-reduced/fully reduced) are very low and comparable to those of ferredoxins [14], whereas the reduction of the quinone form (oxidized) to the semiquinone occurs at much higher midpoint potentials.

Most cyanobacteria studied synthesize flavodoxin, a non-iron electron-transferring protein, when grown under iron-deficient conditions. This FMN-containing protein has been shown to substitute for ferredoxin (both ferredoxin I and II are affected) when the Fe^{3+} concentration in the culture medium is lowered (see Ref. 6). However, this substitution capability varies with the species, even within the same genus [15–17].

The specific interaction of ferredoxin with one subunit of the PS-I reaction center (PSI-D) has been suggested by chemical cross-linking studies [18,19]. Moreover, the inactivation of the gene encoding the PSI-D subunit in *Synechocystis* sp PCC 6803 resulted in an impaired electron transfer to ferredoxin [20]. This transformable cyanobacterium thus appears as a promising tool to investigate the interactions and roles of the different polypeptides present at the reducing side of Photosystem I. In the present work, we show that this cyanobacterium is also capable of replacing ferredoxin by flavodoxin, and we describe the purification procedure and several important biochemical and biophysical properties of these two electron carriers.

Material and Methods

Protein isolation and purification

The cyanobacterium *Synechocystis* sp PCC 6803 was grown photoautotrophically in 16 l batch culture either on BG-11 medium [21] or on BG-11 medium in which the ferric iron concentration was lowered to 8 μM. Cells were collected at late logarithmic phase by continuous centrifugation. Pellets were washed once in 0.4 M sucrose, 10 mM KCl, 50 mM Tricine/NaOH (pH 7.6), 1 mM EDTA. Cells were resuspended in the same buffer containing 1 mM of the following proteinase inhibitors: phenylmethylsulfonyl fluoride, ϵ-amino-*n*-caproic acid and benzamidine. DNAase was also added. The suspension was passed three times through a French pressure cell at 20000 lb/in^2. The homogenate was centrifuged for 10 min at 10000 $\times g$ and the resulting supernatant centrifuged for 1 h at 200000 $\times g$ to sediment the thylakoid membranes. Soluble proteins were isolated following the method of Ho et al. [22], modified as described below. The dark blue supernatant from the last centrifugation was brought to 45% $(NH_4)_2SO_4$ saturation and centrifuged for 20 min at 48000 $\times g$. The blue pellet was discarded and the supernatant was brought to 55% $(NH_4)_2SO_4$ saturation. The precipitated material was collected by centrifugation, resuspended and dialyzed against 20 mM Tricine/NaOH (pH 7.8). The supernatant was successively brought to 70, 90 and 100% $(NH_4)_2SO_4$ saturation. Corresponding pellets were resuspended and dialyzed. The 100% $(NH_4)_2SO_4$ saturation supernatant was loaded onto a DEAE-cellulose (DE 52, Whatman) column equilibrated with saturated $(NH_4)_2SO_4$. The column was first washed with 2 vol. of saturated $(NH_4)_2SO_4$, then 2 vol. of distilled water, and then eluted with 2 M NaCl. The red eluate was then dialyzed, and submitted to FPLC chromatography on an anion exchanger column (Mono Q HR5/5; Pharmacia) equilibrated with 20 mM Tricine/NaOH (pH 7.8) and eluted by a linear NaCl gradient (0–1 M). The dialyzed 90% saturation pellet was also submitted to a similar ion-exchange FPLC. Final purification was achieved by submitting the proteins to a second ion-exchange chromatography and an HPLC gel filtration on a TSK G2000 SW column (LKB) in the same buffer.

Cysteine residue derivatization

Ferredoxin apoproteins were prepared by incubation of the native proteins (100 μM) in 0.1% trifluoroacetic acid, in the presence of a 100-fold molar excess of β-mercaptoethanol. This treatment resulted in the immediate bleaching and precipitation of the proteins. The pellet was dried under vacuum and resolubilized in 6 M guanidinium chloride buffered with 0.1 M Tris-HCl (pH 8.5). β-mercaptoethanol was added to a final concentration of 0.1% to complete the reduction overnight at 4°C.

Chemical modification of cysteine residues was performed by treatment of apo-ferredoxin by 4-vinylpyridine according to Friedman et al. [23]. Apo-ferredoxins in the reducing medium were further incubated for 4 h at room temperature in the presence of a 100-fold molar excess of 4-vinylpyridine relative to cysteine residues. The reaction mixture was then diluted in 50 mM sodium phosphate (pH 7.4), and the reaction was stopped by the addition of dithiothreitol in excess. The *S*-pyridylethylcysteinyl-apo-ferredoxins (PE-apo-ferredoxin) were then extensively dialyzed against 20 mM phosphate buffer (pH 7.4).

Electrophoresis

Analytical slab gel electrophoresis has been designed for the resolution of low molecular mass polypeptides. Gel buffers, sample buffer and acrylamide to bisacrylamide ratio were as described by Laemmli [24], with a final concentration of acrylamide of 6% in the stacking gel and of 15% in the resolving gel. SDS was omitted from the gels. Anode buffer was 0.2 M Tris-HCl (pH 8.9), and cathode buffer was 0.1 M Tris/ 0.1 M

Tricine/ 0.1% SDS, giving a final pH of 8.25 as described by Schägger and Von Jagow [25].

Isoelectric focusing

A 0.5 mm-thick gel was cast, containing 15% acrylamide mixed with carrier ampholyte (Pharmalyte pH 2.5–5). Polymerisation was catalyzed by riboflavin under ultraviolet light. Cathode buffer was 1 M NaOH, and anode buffer was 1 M H_3PO_4. Focusing was performed at constant power (8 W). Protein samples were either in the native state or first incubated in 8 M urea in the presence of 2% β-mercaptoethanol. Gel slices (0.5 × 3 cm) were cut and incubated in water for the measurement of the pH gradient profile along the gel.

Determination of available sulfhydryl groups

Sulfhydryl groups in native ferredoxins were assayed with DTNB (Ellman's reagent) as described by Habeeb [26]. 0.01 μmol of ferredoxin (Fd_p or Fd_s) in 80 mM phosphate buffer (pH 7) and 1 mM EDTA were incubated in the presence of 1 mM DTNB. The color development due to the reaction of DTNB with free thiol groups was followed spectrophotometrically at 410 nm.

Urea gradient gel electrophoresis

0.7 mm-thick slab gels were cast as described by Goldenberg [27]. The transverse urea gradient (0–8 M) was superimposed to an inverse gradient of acrylamide concentration (15–11%) in order to keep electrophoretic mobility of proteins constant. Samples containing native ferredoxins were treated with the electrophoresis sample buffer without reducing agent or incubated 20 h at room temperature in the presence of 8 M urea prior to electrophoresis.

Protein sequencing

PE-apo-ferredoxin$_p$ and PE-apo-ferredoxin$_s$ were cleaved overnight by trypsin (containing residual chymotrypsic activity) or staphylococcal V8 proteinase in 50 mM ammonium carbonate (pH 7.8). Cleaved proteins were dried and solubilized in 0.1% TFA/H_2O, and peptides were purified by reverse-phase HPLC on a Delta-Pak C-18 column (Waters), eluted by a linear gradient of acetonitrile (0–55% (v/v)) in water containing 0.1% (v/v) TFA.

A pulsed liquid sequencer 477A from Applied Biosystems was used for all sequencing assays. Analysis of the phenylthiohydantoin (PTH) derivatives of amino acids was automatically performed by a 120A on-line HPLC analyser (Applied Biosystems).

Potentiometric titrations

The reduction state of the protein was followed spectrophotometrically. Potentiometric measurements were done in an optical cuvette (1 cm optical path), using a platinum plate and a saturated calomel electrode. The cuvette was continuously stirred and flushed with pure argon gas. Ferredoxins were titrated either in 20 mM Tricine/NaOH (pH 8) or in 20 mM glycine/NaOH (pH 9) in the presence of 1 mM KCl and 5 μM benzyl viologen and methyl viologen. Optical measurements were done at 422 and 460 nm. Flavodoxin was titrated in 20 mM Tricine/NaOH (pH 7.3 or pH 8) in the presence of 1 mM KCl, 5 μM of methyl viologen and benzyl viologen, 2 μM of indigo disulfonate, safranine T and anthraquinone-2,6-disulfonate. Optical measurements were done at 464 and 576 nm. The redox potential was adjusted by addition of small volumes of buffered 1 M sodium dithionite or diluted potassium ferricyanide.

Immunological techniques

Antibodies directed against spinach ferredoxin (gift from Dr J.P. Jacquot) were obtained by a classical three-step immunization protocol in the foot pad of five mice (Balb/c). Fluids from Erlich ascites were collected; two of them, exhibiting the highest titers, were used as a pool for general recognition assays.

Dot blot experiments were conducted on nitrocellulose membranes (Bio-Rad). Serial dilutions of the proteins to be tested were quantitatively deposited on the pre-wet membrane with a Bio-Dot apparatus (Bio-Rad) allowing good reproducibility and easy comparison between different dots. Membranes were incubated overnight at 4°C with antisera and the bound antibodies were revealed by an alkaline phosphatase-linked second antibody (Promega).

Results

Fractionated precipitation of the soluble proteins of *Synechocystis* by ammonium sulfate gave results comparable to that described by Ho et al. [22] for other cyanobacterial species. Increasing the ammonium sulfate concentration stepwise from 45 to 100% saturation (steps at 45, 55, 70, 90 and 100%) allowed the removal of most of the blue pigmented proteins in the first steps and greatly simplified the purification of the following fractions. Ferredoxin was detected in the 90% saturation pellet (precipitating Fd: Fd_p) and in the 100% supernatant (soluble Fd: Fd_s). It is worth noting that the intermediate fraction precipitating at 100% saturation was always small, and did not show any detectable absorbance in the visible region. Ion-exchange chromatography of the dialyzed 90% saturation pellet produced two major colored peaks: (1) a bright orange peak (elution at 410 mM NaCl), the visible absorption spectrum of which clearly corresponds to a flavoprotein; (2) a reddish peak corresponding to Fd_p (elution at 500 mM NaCl). In addition, very small

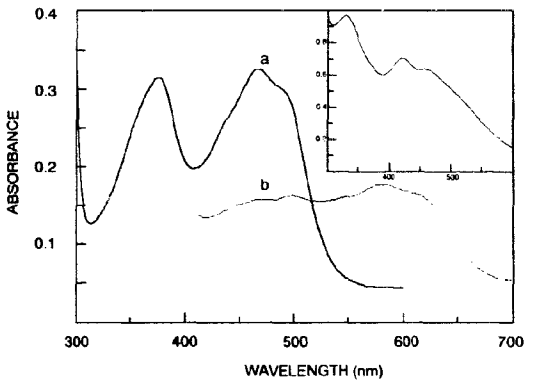

Fig. 1. Absorption spectrum of flavodoxin from *Synechocystis* sp PCC 6803. Flavodoxin was in 20 mM Tricine/NaOH (pH 7.8). (a) oxidized flavodoxin (quinone form). (b) Semi-reduced flavodoxin (semiquinone form) obtained after addition of sodium dithionite. Inset: Absorption spectrum of oxidized ferredoxin (Fd_s) from *Synechocystis* sp PCC 6803 in 20 mM Tricine/NaOH (pH 7.8).

amounts of a reduced *c*-type cytochrome (probably cytochrome c_6) were detected during this purification step. A similar chromatography showed that the 100% saturation supernatant contained almost exclusively ferredoxin (Fd_s, elution at 500 mM NaCl). All the fractions were tested for their reactivity with anti-spinach ferredoxin antibodies. Positive reactions were only observed in the dialyzed 90% pellet and in the 100% supernatant (not shown). In the oxidized state, the purified ferredoxins gave very similar visible absorption spectra showing peaks at 330 nm, 422 nm and 462 nm (Fig. 1, inset). Visible to U–V ratios, A_{330}/A_{276} and A_{422}/A_{276}, typically were about 0.68 and 0.52, respectively. EPR characterization of the ferredoxins in the reduced state gave almost identical spectra, clearly corresponding to a [2Fe-2S] chloroplast-type ferredoxin. EPR *g*-values were 2.05, 1.96 and 1.88 for both Fd_p and Fd_s. Fig. 1 also shows the visible absorption spectra of purified flavodoxin. Peaks at 464 nm and 375 nm in the oxidized state (Fig. 1a) and 576 nm in the semireduced state (Fig. 1b) are characteristic of flavodoxin and are very similar to spectra of other flavodoxins already studied [6]. The A_{464}/A_{280} absorbance ratio for purified flavodoxin was typically about 0.25.

When cells grown under iron deficiency were used, ferredoxin was no longer detectable, neither in the 90% saturation pellet, nor in the 100% saturation supernatant, and the amount of flavodoxin in the 90% saturation pellet was greatly increased.

The yields of pure proteins (ferredoxin under normal growth conditions and flavodoxin under iron deficiency) were about 15–20 nmol per litre of culture for both ferredoxin and flavodoxin.

Redox titrations of ferredoxins were followed by measuring their visible absorbance either at 422 nm or at 460 nm (Fig. 2). Small amounts of viologens did not contribute to the absorbance at these wavelengths. Both reductive and oxidative titrations were done and gave identical results. Nernst plots of the data indicate that *Synechocystis* ferredoxins undergo a one electron redox transition ($n = 1$). The midpoint potential for both the Fd_s and the Fd_p was found to be $E_m = -0.412 \pm 0.005$ V at pH 9 and pH 8 (not shown). Calculation of potentials at pH 8 was slightly less satisfactory since, at this pH value, the complete reduction of ferredoxins was barely achieved with dithionite, and thus the estimate of the absorbance value of totally reduced ferredoxins was less accurate. However, both proteins did not show any significant variation of their E_m between pH 8 and pH 9.

Flavodoxin redox titrations were followed either at 576 nm (absorbance due to the semiquinone species) or at 464 nm (absorbance due to both quinone and semiquinone forms), at pH 7.3 or pH 7.8. Fig. 3A shows the bell-shaped titration curves measured at 576 nm. These curves correspond to the formation of the semiquinone and to its transformation into the fully

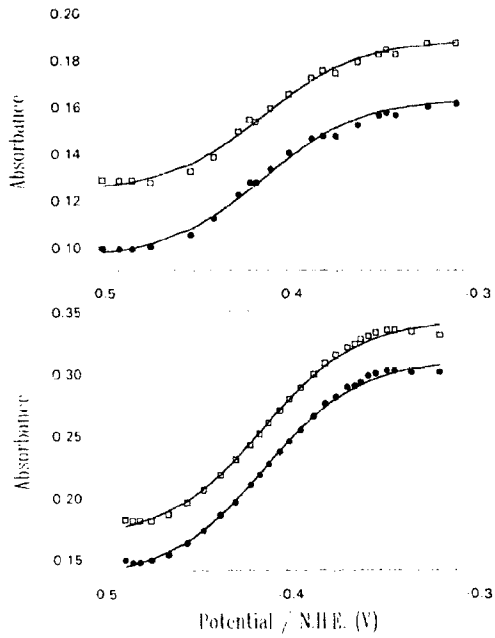

Fig. 2. Ferredoxin redox titration at pH 9 in 20 mM glycine/NaOH, 1 mM KCl, in the presence of 5 μM benzyl viologen and 5 μM methyl viologen. The optical cuvette (1 cm optical path) was stirred and continuously flushed with pure argon gas. Upper panel: titration of Fd_p. Lower panel: titration of Fd_s. (□): absorbance measurement performed at 422 nm. (●): absorbance measurements performed at 460 nm. The solid lines are theoretical titration curves for a one-electron reaction according to the Nernst equation.

reduced quinol form. Both transitions correspond to a one electron reaction ($n = 1$). Fittings of the data according to Nernst equation indicate $E_{m1} = -0.428$ V and $E_{m2} = -0.216$ V at pH 7.3, and $E_{m1} = -0.438$ V and $E_{m2} = -0.238$ V at pH 7.8. Fig. 3B shows the two redox transitions of flavodoxin titration measured at 464 nm. At this wavelength, the high-potential transition corresponds to a larger absorbance change than at 576 nm. Data fitting according to Nernst equation indicate that both transitions involve a single electron and potentials are $E_{m1} = -0.426$ V and $E_{m2} = -0.217$ V at pH 7.3, and $E_{m1} = -0.433$ V and $E_{m2} = -0.238$ V at pH 7.8. Variation of the high midpoint potential value (E_{m2}) with the pH value of the medium corresponds to 45 mV per pH unit. Although low, this value probably indicates that the first redox transition involves one proton and one electron, and thus has an E_m which decreases by 59 mV per pH unit. E_{m1} value also showed a slight decrease upon pH increase (12 mV per pH unit), but this variation was within the limits of experimental errors, and could not be considered as significant. Extensive studies of pH effects on E_m of various algal and cyanobacterial flavodoxins have been performed by Sykes and Rogers [14]. They showed that E_{m1} (low potential value) is pH insensitive, whereas E_{m2} varies by 59 mV per pH unit. In this respect *Synechocystis* flavodoxin appears to show similar oxido-reduction properties.

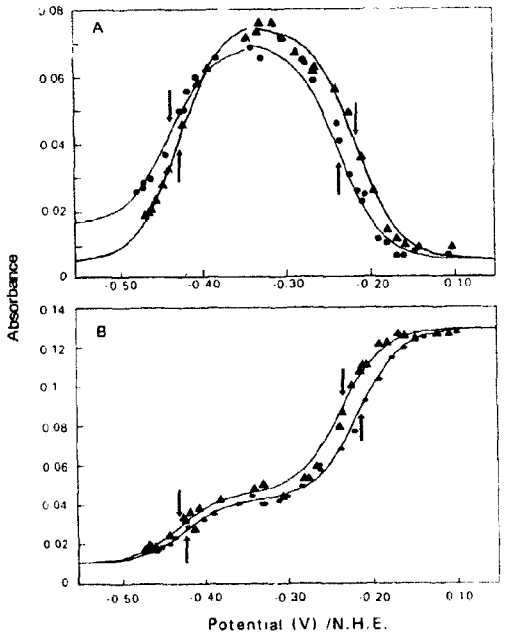

Fig. 3. Flavodoxin redox titration: (A) in 20 mM Tricine/NaOH pH 7.3 (▲) or pH 7.8 (●) in the presence of 1 mM KCl, 5 μM of benzyl viologen and methyl viologen, 2 μM of indigo disulfonate, safranine T and anthraquinone 2,6-disulfonate. Absorbance measurements were performed at 576 nm. Other conditions as in Fig. 2. (B) at pH 7.3 (▲) or pH 7.8 (▲). Absorbance measurements were performed at 464 nm. Solid lines are theoretical titration curves for two successive one-electron reactions according to the Nernst equation. Arrows indicate the midpoint potentials.

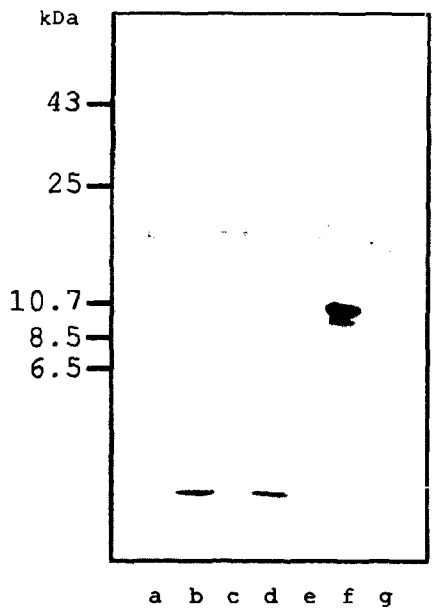

Fig. 4. SDS-PAGE of spinach Fd (lane a), *Synechocystis* 6803 Fd_p and Fd_c, in their native (lanes b and d) and PE-derivatized form (lanes c and e), respectively, and *Synechocystis* 6803 flavodoxin in native and reduced form, respectively (lanes f and g).

On SDS-PAGE, native ferredoxins (in the absence of a reducing agent) showed unusually high electrophoretic mobility (Fig. 4, lanes b and d). This corresponds to a very low apparent molecular mass, close to 2 kDa and strictly identical for both ferredoxins. When SDS-PAGE was performed in the presence of 6 M urea, the apparent molecular mass was increased by 1.5 kDa for both ferredoxins (see Fig. 5). After full derivatization of cysteines, mobility of the PE-apo-ferredoxins was greatly reduced, showing a single band with an apparent molecular mass of 16.5 kDa (Fig. 4, lanes c and e). Control spinach ferredoxin exhibited a much simpler electrophoretic behavior, since, even without any preliminary reduction of the cysteines, the iron-sulfur cluster was probably lost during the course of SDS-PAGE, giving a single band corresponding to an apparent molecular mass of 17.5 kDa (Fig. 4, lane a). Flavodoxin was first analysed in the absence of any reducing agent in the sample buffer. A main band was observed with an apparent molecular mass of 9.5 kDa: a slightly faster migrating component was also visible in an overloaded sample (Fig. 4, lane f). Upon addition of 5% β-mercaptoethanol to the sample buffer, one single

band remained, with a higher apparent molecular mass of 15.0 kDa (Fig. 4, lane g).

The influence of urea on the electrophoretic migration of ferredoxin from *Synechocystis* was further investigated using electrophoresis in the presence of a transverse gradient of this denaturing agent. Native proteins showed a change in electrophoretic mobility between 4 and 5 M urea as illustrated in the case of Fd_p (Fig. 5). The upper band (at 3.5 kDa) observed at high urea concentration remained diffuse, without continuity with the lower band. No staining was detected at the level of the fully denatured protein (16.5 kDa). Samples incubated overnight at 20°C in the presence of 8 M urea showed a somewhat different pattern. A continuous band was present at 13.0 kDa, migrating slightly faster than the fully unfolded PE-apo-Fd. This is probably due to some irreversible structural changes, resulting from the loss of the iron-sulfur cluster. However a major fraction of the protein was still in the native form, giving a pattern close to that observed when the sample was not incubated overnight. In this case, the intermediate band at 3.5 kDa appeared sharper, but the transition back to the native state occurred at almost the same urea concentration as the reverse process. Similar results were observed with Fd_p and Fd_s (not shown).

Isoelectric points of *Synechocystis* Fd_s, Fd_p and flavodoxin, were measured in the native state or after incubation in the presence of 8 M urea and 2% β-mercaptoethanol. Spinach plastocyanin and spinach ferredoxin were used as control samples. Results are summarized in Table I. The spinach plastocyanin isoelectric point was found to be $pI = 4.22$ in the native state, in good agreement with the values ($pI = 4.2$) reported by Katoh et al. [28] and Ramshaw et al. [29]. In the native state, ferredoxins from *Synechocystis* appeared to precipitate during the course of the migration. After incubation in the presence of urea and β-mercaptoethanol, Fd focused as a sharp band. Isoelectric points are identical for both Fd_p and Fd_s ($pI = 3.48$). Native flavodoxin isoelectric point ($pI = 3.76$) is in the range of values reported by Dutton and Rogers [30] for *Nostoc* MAC ($pI = 3.49$) and *Chondrus crispus* ($pI = 3.51$) flavodoxins.

TABLE I

Isoelectric points

Treated samples were incubated in the presence of urea and β-mercaptoethanol; n.d. not determined.

Samples	Spinach plastocyanin	Flavodoxin	Spinach Fd	Fd_p	Fd_s
Native	4.22	3.76	n.d.	n.d.	n.d.
Treated	4.32	4.00	3.69	3.48	3.48

Fd_s and Fd_p were further compared on the basis of their reactivity towards antibodies raised against spinach ferredoxin. Serial dilutions of both native and PE-apo-ferredoxins from *Synechocystis* were tested in a dot-blot experiment, together with native spinach

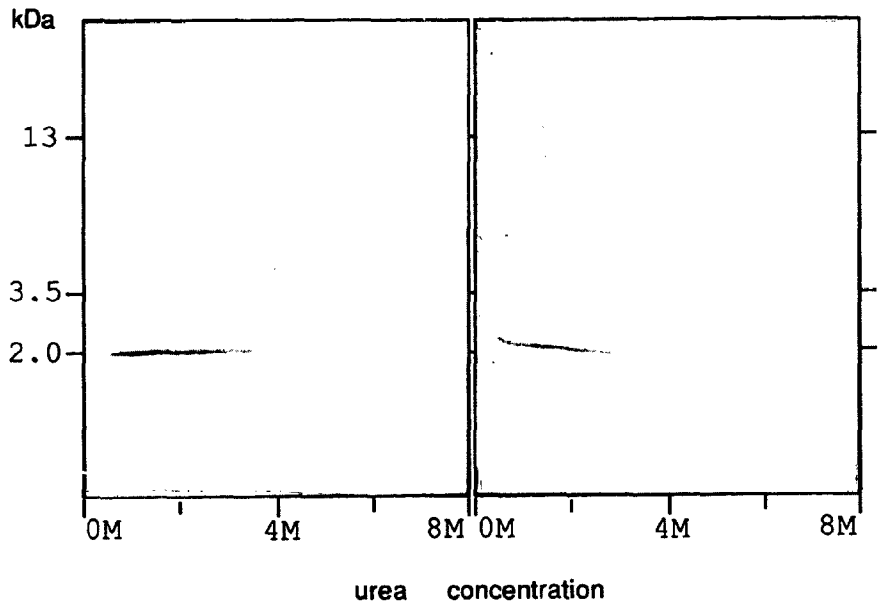

Fig. 5. Urea gradient gel electrophoresis of Fd_p. Total run length was 4 h. Linear deposits on full gel width were made with a native protein (left gel), and with a similar sample after 20 h incubation in 8 M urea at 20°C (right gel).

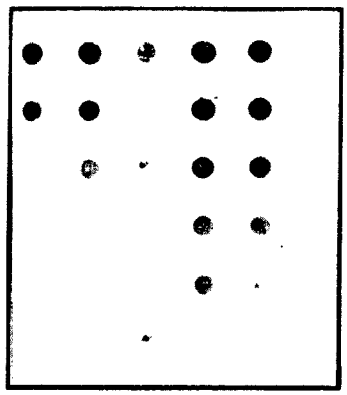

Fig. 6. Ferredoxins comparison by dot immunoblotting. Two-fold decreasing amounts of protein were successively loaded in each well. Highest amounts were: 0.1 nmol for native and PE-apo-Fd_p (a, b), native and PE-apo-Fd_s (c, d) and control native horse heart cytochrome *c* (f), and 0.04 nmol for native spinach Fd (e). Concentrations were based on amino-acid analysis.

ferredoxin. Whether native or derivatized, Fd_p showed high and similar reactivities (Fig. 6 lanes a and b). This was not the case for native Fd_s (lane c) which was about 5-times less efficiently recognized than native Fd_p. After full derivatization of cysteine residues, PE-apo-Fd_s (lane d) was as efficiently recognized as PE-apo-Fd_p. The best reactivities for both *Synechocystis* ferredoxins was about 6-times lower than the control spinach ferredoxin (Fig. 6, lane e).

Full amino-acid sequences have been obtained for both Fd_p and Fd_s, based on the combined sequencing of N-terminal end and various proteolytic peptides purified by reverse phase chromatography (Fig. 7). All reactions were conducted on the PE-apo-proteins, allowing a clear identification of the cysteine derivative during the final sequencing step. Sequences of Fd_p and Fd_s appeared to be strictly identical and gave a calculated molecular mass of 10232 Da (apo-ferredoxin).

Free thiol assays were performed on spinach and *Synechocystis* ferredoxins using DTNB. In spinach ferredoxin, DTNB reaction indicated one free thiol group per protein molecule, whereas, under the same

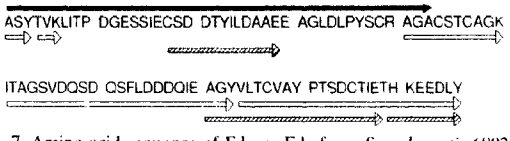

Fig. 7. Amino acid sequence of Fd_p or Fd_s from *Synechocystis* 6803. Overlapping sequences were obtained either from N-terminal direct sequencing (black arrow), or peptides from V8 proteolysis (dashed arrows) or trypsic/chymotrypsic proteolysis (open arrows).

conditions, no reaction was detected with *Synechocystis* ferredoxin. The reaction was also negative after incubation of the protein in 6 M urea.

Direct N-terminal sequencing was performed on flavodoxin, giving a 42-amino-acid sequence, with some uncertainties remaining at positions 24 and 34 (see Fig. 9a).

Discussion

A [2Fe-2S] ferredoxin has been found in *Synechocystis* 6803. It has been isolated following the method described by Ho et al. [22] for other cyanobacteria. Most of the ferredoxin is found in the saturated ammonium sulfate supernatant (Fd_s) and a small amount is also present in the 90% saturation pellet (Fd_p). However, the occurrence of Fd in two distinct fractions does not reflect the existence of two different proteins as in many other cyanobacterial genera [6–8]. In the case of *Synechocystis* 6803, most biophysical characteristics such as EPR spectra, absorption spectra and redox titrations appeared to be identical for ferredoxins from both fractions. This is further documented by the identity of the full primary sequences, giving a calculated molecular mass of 10232 Da (apo-ferredoxin). Electrophoretic migration of these proteins is unusually high, and varies greatly with their folding state. In the absence of any reducing agent, they apparently keep a tightly folded conformation, leading to a dramatic underestimate of the apparent molecular mass. The presence of a denaturing agent during electrophoresis (6 M urea) led to an increase of this apparent molecular mass from 2.0 to 3.5 kDa. A similar action of urea has been already reported for spinach ferredoxin [11]. In this case, the transition was observed at a urea concentration of 4 M. For *Synechocystis* 6803 ferredoxin, these two types of migration were clearly compared by transverse urea gradient electrophoresis (Fig. 5), the transition then occurring between 4 and 5 M urea. The absence of a clear continuity between the two bands when the sample is initially in the presence of urea can be indicative of a slow conversion between two folding states of the protein [27]. After prolonged preincubation in 8 M urea, a third band appeared at 13 kDa (Fig. 5), which did not undergo transitions to the other folding states, even at low urea concentration. It is probably due to the irreversible loss of the iron-sulfur cluster. Indeed, this 13 kDa band was observed in samples in which the cluster has been removed by acidic treatment (0.1 % TFA, data not shown). Upon reduction of the same sample by β-mercaptoethanol, this 13 kDa band was transformed into a 16.5 kDa band, as observed with the fully derivatized protein (PE-apo-ferredoxin, Fig. 4, lane c). So, on SDS-PAGE, ferredoxin shows four different states: folded (2 kDa, native state), partly unfolded (3.5

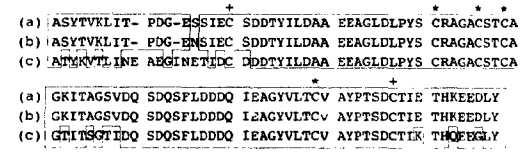

Fig. 8. Comparison of amino acid sequences of cyanobacterial [2Fe-2S] ferredoxins. Gaps are inserted to give maximum homology. * indicates cysteine residue ligated to the iron-sulfur cluster. + indicates additional cysteine residue. The sequences are from (a) *Synechocystis* sp PCC 6803 (this work), (b) *Synechocystis* sp PCC 6714 (Ref. 32), (c) *Spirulina platensis* (Ref. 2).

kDa), apo-ferredoxin (13 kDa, no cluster) and unfolded apo-ferredoxin (16.5 kDa, no cluster and cysteines totally reduced or chemically blocked).

The reactivities of the two *Synechocystis* Fd with antibodies directed against spinach ferredoxin are clearly different. Native Fd_s produced a faint signal in dot blot assays as compared to native Fd_p. Since a comparable reactivity was recovered by the unfolding of the protein (PE-apo-Fd_s), we conclude that a slight difference between the conformation of the two native proteins exists, leaving most physico-chemical properties unaffected, but detectable by very sensitive techniques such as the binding of antibodies. Further studies on the precipitating ferredoxin (Fd_p) are impeded by its low abundance (at least 10-times lower than Fd_s).

Oxidoreduction potential of *Synechocystis* 6803 ferredoxin (from both fractions) ($E_m = -412$ mV) is more negative than the potential of other cyanobacterial ferredoxins (except ferredoxin II from *Nostoc* MAC) [6] and lies in the potential range of higher plant ferredoxins [31].

Fig. 8 shows the sequence alignment of ferredoxins from *Synechocystis* 6803, *Synechocystis* 6714 [32] and *Spirulina platensis* [2]. Ferredoxins from both *Synechocystis* strains are 96 amino acids long and differ only by one residue (Ser-16 replaced by Asn). *Spirulina platensis* ferredoxin is slightly longer (98 amino acids) and its identity with *Synechocystis* 6803 is 80%. The differences are mostly located at the amino-terminal end (positions 2–21), in the middle of the sequence (positions 52–58) and near the carboxy-terminal end (positions 90–96). These three regions have already been shown to be the most variable segments of chloroplast-type ferredoxins [2]. The high conservation of the region including the four cysteine residues binding the iron-sulfur cluster (Cys-41, Cys-46, Cys-49 and Cys-79) is also a common feature of the ferredoxin molecules.

Considering the 40 sequences of chloroplast-type ferredoxins already determined, it appears that they contain either four, five (the additional one being either Cys-20 or Cys-87) or six cysteine residues (both Cys-20 and Cys-87). The sequence of *Euglena viridis* ferredoxin shows that this protein contains 7 cysteine residues [33], but up to now, it is the only known example. The group of species having ferredoxins with six cysteine residues contains no higher plant Fd, and almost exclusively cyanobacterial Fd (including *S. platensis* and *Synechocystis* 6803) and only two green algae *Scenedesmus quadricauda* and *Chlamydomonas reinhardtii*. When absent, Cys-20 is always replaced by a valine residue, whereas Cys-87 is frequently replaced by a valine residue, or less frequently by an alanine or a leucine residue [2]. The classification of Fd according to the number of cysteine residues present in their sequences has no obvious phylogenetic significance, but it could be interesting to look for correlations between electrophoretic behavior or stability and the presence of both Cys-20 and Cys-87.

Computer-assisted visualisation of *S. platensis* crystal structure clearly shows that Cys-20 and Cys-87 are in close vicinity. However, in the crystal, the distance between the two sulfur atoms of Cys-20 and Cys-87 is too large (about 8.8 Å) to allow the formation of a disulfide bridge. *Synechocystis* 6803 Fd shows no thiol group reacting with DTNB even when incubated in 6 M urea. On the contrary, in spinach Fd which contains only five cysteine residues, one fast reacting thiol group is detected (probably due to Cys-20). The high stability, the high electrophoretic mobility of *Synechocystis* 6803 Fd together with its absence of reactivity towards free thiol reactant leads us to propose the possibility of a disulfide bridge between Cys-20 and Cys-87. This additional constraint would provide a more compact and stable structure in the absence of reducing agent.

In *Synechocystis* 6803, flavodoxin is normally found in very small amounts. Its appearance in the cells can be due to a progressive iron deficiency taking place during the growth, at the end of the logarithmic phase. Iron deficiency is known to induce flavodoxin synthesis in many cyanobacteria. We show that this is also the case for *Synechocystis* 6803 grown in the presence of a low iron concentration. Under such growth conditions, ferredoxin is no longer detected and the amount of flavodoxin is greatly increased. The midpoint potentials of *Synechocystis* 6803 flavodoxin show values close to those already reported for other cyanobacterial flavodoxins [6].

Fig. 9 shows that the amino-terminal sequence of *Synechocystis* 6803 flavodoxin has a high degree of homology with the long-chain flavodoxins (type II) isolated from *Synechococcus* sp PCC 6301 (*Anacystis nidulans*) [34], *Nostoc* MAC [35], *Anabaena* sp PCC 7119 (not shown) [17] and, to a lesser extent, with the flavodoxin from the eukaryotic red alga *Chondrus crispus* [36]. Considering the first 36 amino acids, *Synechocystis* 6803 flavodoxin has 69% identity with *Synechococcus* sp PCC 6301, 53% with *Nostoc* MAC and

(a) -MKIGLFYGTQTGNTETIAELIQK?MGGDSVVDM?DISQAADV
(b) -AKIGLFYGTQTGVTQTIAESIQQEFGGESIVDLNDIANADAS
(c) SKKIGLFYGTQTGKTESVAEII-DEFGDEVVTLDID
(d) --KIGIFFSTSTGNTTEVADFIGKTLGAKASAPISV

Fig. 9. Comparison of the amino-terminal amino -acid sequence of *Synechocystis* 6803 flavodoxin with flavodoxins from other cyanobacteria and a red alga. Sequences are from (a) *Synechocystis* sp PCC 6803 (this work), (b) *Synechococcus* sp PCC 6301 [34]. (c) *Nostoc* MAC [35] (d) *Chondrus crispus* [36]. Gaps are inserted to give maximum homology. Underlined residues correspond to ambiguous amino acid determination. Question marks replace amino acids which are still uncertain.

37% with *Chondrus crispus* flavodoxins respectively. These values are even higher if comparison is restricted to the part extending from positions 3–17 (numbering relates to *Nostoc* sequence), which includes a noticeable threonine-rich segment. Crystal structure analysis of flavodoxins from *Synechococcus* 6301 [34] and *Chondrus crispus* [37] has clearly shown the involvement of the N-terminal part of the protein in the interaction with the phosphate of the FMN prosthetic group.

Although the N-terminal sequences of long-chain and short-chain (type I) flavodoxins show some homologies, the highly conserved sequence extending from amino acid 1 to 15 is clearly different between these two groups. The N-terminal ends of short-chain flavodoxins from the anaerobic bacteria *Clostridium* MP, *Clostridium pasteurianum*, *Desulfovibrio vulgaris* and *Peptostreptococcus elsdenii* have in common the conserved sequence ...IVVW/GSGTGNTE... which is not observed in long-chain flavodoxins [13]. So we propose, from the amino-acid sequences comparisons, that *Synechocystis* 6803 flavodoxin is a long-chain (type II) flavodoxin, despite its low apparent molecular mass.

Acknowledgments

We are specially grateful to Dr. A. Menez and F. Bouet for unlimited use of the sequencing facilities. We also greatly appreciated the contribution of Dr. Y. Frobert in the antibodies production. We thank Dr. P. Sétif for EPR spectroscopy of ferredoxins, and Ms. S. Andrianambinintsoa and D. Dejonghe for expert technical assistance. A part of this work was supported by CNRS (URA 1290).

References

1 Knaff, D.B. and Hirasawa, M. (1991) Biochim. Biophys. Acta 1056, 93–125.
2 Fukuyama, K., Hase, T., Matsumoto, S., Tsukihara, T., Katsube, Y., Tanaka, N., Kakudo, M., Wada, K. and Matsubara, H. (1980) Nature 286, 522–524.
3 Tsukihara, T., Fukuyama, K., Nakamura, M., Katsube, Y., Tanaka, N., Kakudo, M., Wada, K., Hase, T. and Matsubara, H. (1981) J. Biochem. 90, 1763–1773.
4 Tsutsui, T., Tsukihara, T., Fukuyama, K., Katsube, Y., Hase, T., Matsubara, H., Nishikawa, Y. and Tanaka, N. (1983) J. Biochem. 94, 299–302.
5 Rypniewski, W.R., Breiter, D.R., Benning, M.M., Wesenberg, G., Oh, B.-H., Markley, J.L., Rayment, I. and Holden, H.M. (1991) Biochemistry 30, 4126–4131.
6 Rogers, L.J. (1987) in The Cyanobacteria (Fay, P. and Van Baalen, C., eds.) pp. 35–67, Elsevier, Amsterdam.
7 Cohn, C.L., Alam, J. and Krogmann, D.W. (1985) Physiol. Vég. 23, 659–667.
8 Matsubara, H. and Wada, K. (1988) Methods Enzymol. 167, 387–410.
9 Wada, K., Oh-Oka, H. and Matsubara, H. (1985) Physiol. Vég. 23, 679–686.
10 Sakihama, N. and Shin, M. (1987) Arch. Biochem. Biophys. 256, 430–434.
11 Ohmori, D., Hasumi, H., Yamakura, F., Murakami, M., Fujisawa, K., Taneoka, Y. and Yamamura, T. (1989) Biochim. Biophys. Acta 996, 166–172
12 Kimata, Y. and Hase, T. (1989) Plant Physiol. 89, 1193–1197
13 Mayhew, S.G. and Ludwig, M.L. (1975) in The Enzymes (Boyer, P.D. ed.), 3rd Edn., Vol. 12, pp. 57–118, Academic Press, New York.
14 Sykes, G.A. and Rogers, L.J. (1984) Biochem. J. 217, 845–850.
15 Pardo, M.B., Gomez-Moreno, C. and Peleato, M.L. (1990) Arch. Microbiol. 153, 528–530.
16 Fillat, M.F., Sandman, G. and Gomez-Moreno, C. (1988) Arch. Microbiol. 150, 160–164.
17 Fillat, M.F., Edmonson, D.E. and Gomez-Moreno, C. (1990) Biochim. Biophys. Acta 1040, 301–307.
18 Zanetti, G. and Merati, G. (1987) Eur. J. Biochem. 169, 143–146.
19 Zilber, A.L. and Malkin, R. (1988) Plant Physiol. 88, 810–814.
20 Chitnis, P.R., Reilly, P.A. and Nelson, N. (1989) J. Biol. Chem. 264, 18381–18385.
21 Rippka, R., Déruelles, J., Waterbury, J.B., Herdman, M. and Stanier, R.Y. (1979) J. Gen. Microbiol. 111, 1–61.
22 Ho, K.-K., Ulrich, E.L., Krogmann, D.W. and Gomez-Lojero, C. (1979) Biochim. Biophys. Acta 545, 236–248.
23 Friedman, M., Krull, L.H. and Cavins, J.F. (1970) J. Biol. Chem. 245, 3868–3871.
24 Laemmli, U.K. (1970) Nature 227, 680–685.
25 Schägger, H. and Von Jagow, G. (1987) Anal. Biochem. 166, 368–379.
26 Habeeb, A.F.S.A. (1972) Methods Enzymol. 25, 457–464.
27 Goldenberg, D.P. (1990) in Protein structure: a practical approach (Creighton, T.E., ed.), pp. 225–250, IRL Press, Oxford.
28 Katoh, S. and Takamiya, A. (1962) J. Biochem. 51, 32–40.
29 Ramshaw, J.A.M., Brown, R.H., Scawen, M.D. and Boulter, D. (1973) Biochim. Biophys. Acta 303, 269–273.
30 Dutton, J.E. and Rogers, L.J. (1978) Biochim. Biophys. Acta 537, 501–506.
31 Cammack, R., Rao, K.K., Bargeron, C.P., Hutson, K.G., Andrew, P.W. and Rogers, L.J. (1977) Biochem. J. 168, 205–209.
32 Hase, T., Inoue, K., Matsubara, H., Williams, M.M. and Rogers, L.J. (1982) J. Biochem. 92, 1357–1362.
33 Ambler, R.P., Kamen, M.D., Bartsch, R.G. and Meyer, T.E. (1991) Biochem. J. 276, 47–52.
34 Smith, W.W., Pattridge, K.A., Ludwig, M.L., Petsko, G.A., Tsernoglou, D., Tanaka, M. and Yasunobu, K.T. (1983) J. Mol. Biol. 165, 737–755.
35 Takruri, I., Boulter, D., Fitzgerald, M.P., Hutber, G.N. and Rogers, L.J. (1986) Phytochem. 25, 2113–2115.
36 Wakabayashi, S., Kimura, T., Fukuyama, K., Matsubara, H. and Rogers, L.J. (1989) Biochem. J. 263, 981–984.
37 Fukuyama, K., Wakabayashi, S., Matsubara, H. and Rogers, L.J. (1990) J. Biol. Chem. 265, 15804–15812.